Chemisorbed and Physisorbed Structures for 1,10-Phenanthroline and Dipyrido[3,2-*a*:2',3'-*c*]phenazine on Au(111)

Peter F. Cafe[a], Allan G. Larsen,[a] Wenrong Yang,[a] Ante Bilic[a], Iain M. Blake[a], Maxwell J. Crossley[a], Jingdong Zhang[b], Hainer Wackerbarth[b], Jens Ulstrup[b], and Jeffrey R. Reimers[a]*

[a] School of Chemistry, The University of Sydney, NSW, 2006, Australia

[b] Department of Chemistry and NanoDTU, Technical University of Denmark, DK-2800 Lyngby, Denmark

1. Full version of References

(27)   "Gaussian 03, Revision B.02" Frisch, M. J.; Trucks, G. W.; Schlegel, H. B.; Scuseria, G. E.; Robb, M. A.; Cheeseman, J. R.; Montgomery, J. A.; Vreven, T.; Kudin, K. N.; Burant, J. C.; Millam, J. M.; S., I. S.; Tomasi, J.; Barone, V.; Mennuci, B.; Cossi, M.; G., S.; N., R.; Petersson, G. A.; Nakatsuji, H.; Hada, M.; Ehara, M.; Toyota, K.; Fukuda, R.; Hasegawa, J.; Ishida, M.; Nakajima, T.; Honda, Y.; Kitao, O.; Nakai, H.; Klene, M.; Li, X.; Knox, J. E.; Hratchian, H. P.; Cross, J. B.; Adamo, C.; Jaramillo, J.; Gomperts, R.; Stratmann, R. E.; Yazyev, O.; Austin, A. J.; Cammi, R.; Pomelli, C.; Ochterski, J. W.; Ayala, P. A.; Morokuma, K.; Voth, G. A.; Salvador, P.; Dannenberg, J. J.; Zakrzewski, V. G.; Dapprich, S.; Daniels, A. D.; Strain, M. C.; Farkas, O.; Malick, D. K.; Rabuck, A. D.; Raghavachari, K.; Foresman, J. B.; Ortiz, J. V.; Cui, Q.; Baboul, A. G.; Clifford, S.; Cioslowski, J.; Stefanov, B. B.; Liu, G.; Liashenko, A.; Piskorz, P.; Komaromi, I.; Martin, R. L.; Fox, D. J.; Keith, T.; Al-Laham, M. A.; Peng, C. Y.; Nanayakkara, A.; Challacombe, M.; Gill, P. M. W.; Johnson, B. G.; Chen, W.; Wong, M. W.; Gonzalez, C.; Pople, J. A. *Gaussian 03, Revision B.02*; Gaussian, Inc., Pittsburgh PA, 2003.

(28)   "TURBOLMOLE-4.0" Ahlrichs, R.; Bär, M.; Baron, H. P.; Bauernschmitt, R.; Böcker, S.; Ehrig, M.; Eichkorn, K.; Elliot, S.; Haase, F.; Häser, M.; Horn, H.; Huber, C.; Huniar, U.; Kattannek, M.; Kölmel, C.; Kollwitz, M.; Ochsenfeld, C.; Öhm, H.; Schäfer, A.; Schneider, U.; Treutler, O.; von Arnim, M.; Weigend, F.; Weis, P.; Weiss, H. *TURBOLMOLE-4.0*; Quantum Chemistry Group: University of Karlsruhe, 1997.

(30)   "Molcas Version 5" Andersson, K.; Barysz, M.; Bernhardsson, A.; Blomberg, M. R. A.; Cooper, D. L.; Fleig, T.; Fülscher, M. P.; Gagliardi, C. d.; Hess, B. A.; Karlström, G.; Lindh, R.; Malmqvist, P.-Å.; Neogrády, P.; Olsen, J.; Roos, B. O.; Sadlej, A. J.; Schütz, M.; Schimmelpfennig, B.; Seijo, L.; Serrano-Andrés, L.; Siegbahn, P. E. M.; Stålring, J.; Thorsteinsson, T.; Veryazov, V.;

Widmark, P.-O. *Molcas Version 5*; University of Lund: Lund, 2000.

2. STM images of phenanthroline obtained under electrochemical potential control

This section provides further STM images of the bare gold surface and the phenanthroline monolayers formed on it. The images were taken over a 10 hour period, with the images presented in Figure 2 being obtained towards the end of this period. The drift of the STM tip reduced continually during this period as the instrument stability increases. Figure S1 shows two successive scans of the bare surface, each scan imaged in the opposite direction: the gold ($\sqrt{3} \times 22$) R30° reconstruction is readily identified in these images, and the image drift, even at this early stage of experimentation is clearly identified. The observed spacing between the reconstruction lines is used to calibrate the instrument. Soon after addition of the phenanthroline into solution, monolayers appeared on the surface as short chains of stacked phenanthrolines whose structure evolved rapidly with time as shown in Figure S2. However, the long-range order increased gradually, with typical long-time configurations displayed in Fig. 4. Occasionally, extended regions of high order are seen such as those displayed in Fig. S3. High resolution images indicate a surface coverage of 2.5±0.1 molecules nm^{-2} as expected for a (4 × 4) lattice. The images shown in Figure S3 were obtained using feedback conditions ($I = 5.0$ and $P = 5.0$) typical of constant-height STM scanning, but do not achieve sum-the molecular resolution needed to identify the molecular orientation. To obtain the resolution required for this identification, the feedback was reduced ($I = 0.6$ and $P = 1.0$). Although this reduction results in contamination of the otherwise pure differential current-deviation image, the resolution of increased sufficient to observe the molecular plane and hence allow the full characterization of the structures given in Table 1.
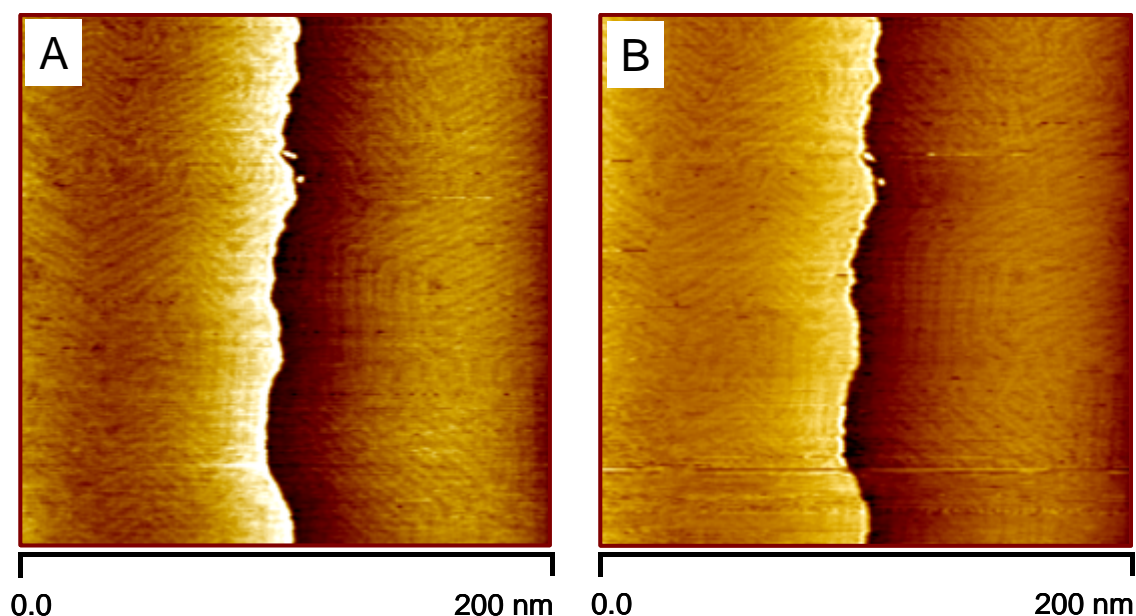

Figure S1: Two successive current images of the bare Au(111) surface, scanned in alternate directions, obtained in constant-current scanning mode at a set-point current I_t=0.15 nA, nA, V_{bias} = -0.1 V and E_w= -0.6 V vs. SCE.
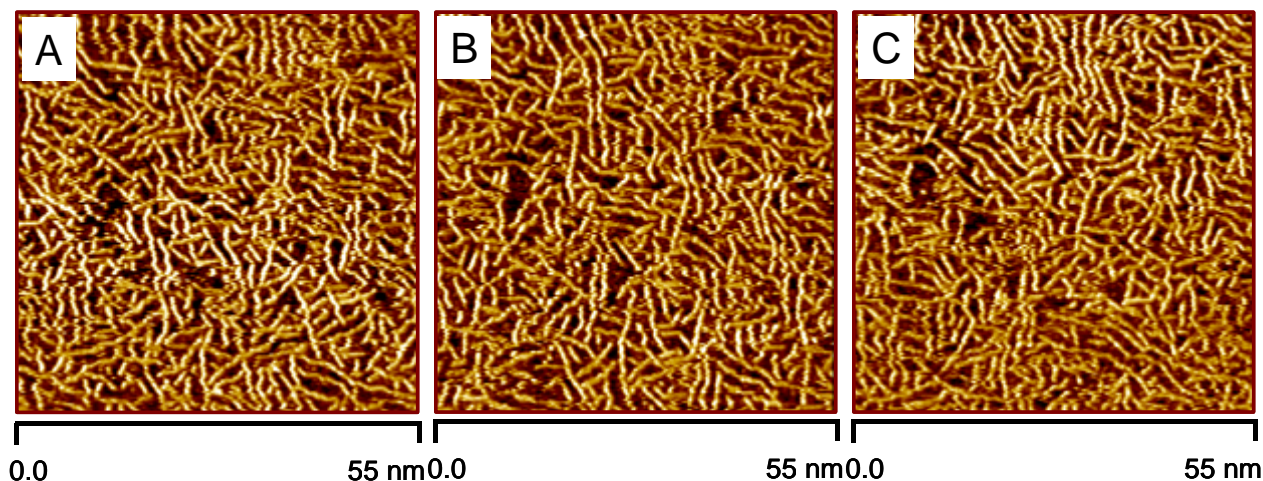
Figure S2: Three successive current images of phenanthroline on Au(111) surface during the early stages of monolayer formation, scanned in alternate directions, obtained in constant-current scanning mode at a set-point current of $I_t = 0.60$ nA, V_{bias}=-0.55 V and $E_w = 0.03$ V vs. SCE.

Precise definitions of the quantities used in performing the in situ STM experiments are:

1. V_{bias} = difference in potential between the tip and the working electrode.

2. I_t is set-point tunnelling current from tip to substrate (in these experiments, the substrate is also the working electrode).

3. E_w is the difference in potential between the working electrode and the reference electrode. It is corrected to be vs SCE.

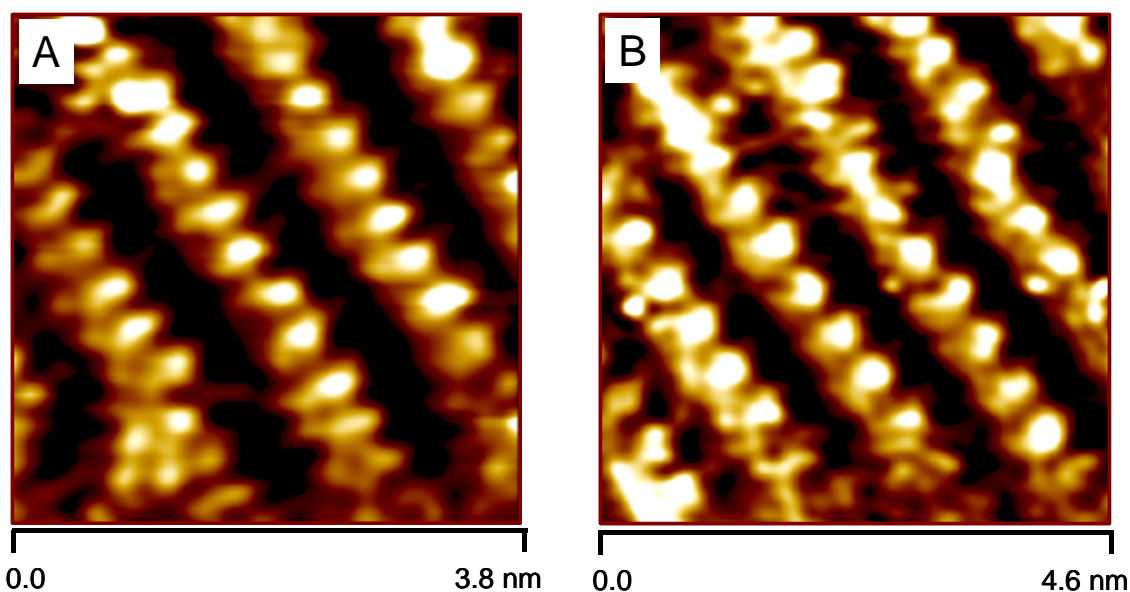4. E_t is the difference in potential between the tip and the reference electrode.

Figure S3: Two successive current images of phenanthroline on gold(111) surface, scanned in alternate directions, obtained in constant-current scanning mode $I_t = 0.85$ nA, $V_{bias} = -0.607$ V and $E_w = 0.08$ V vs. SCE.

Three images of the monolayer formed in situ are shown in Fig. S4. The upper of these images is that shown in Fig. 2 while the following images show regions of the surface that overlap in the vertical direction. The blue lines show the boundaries between different regions on the surface, while the number of PHEN molecules per chain in each region (in order 9, 3, 6, 3, 6, 3, 3) is indicated.
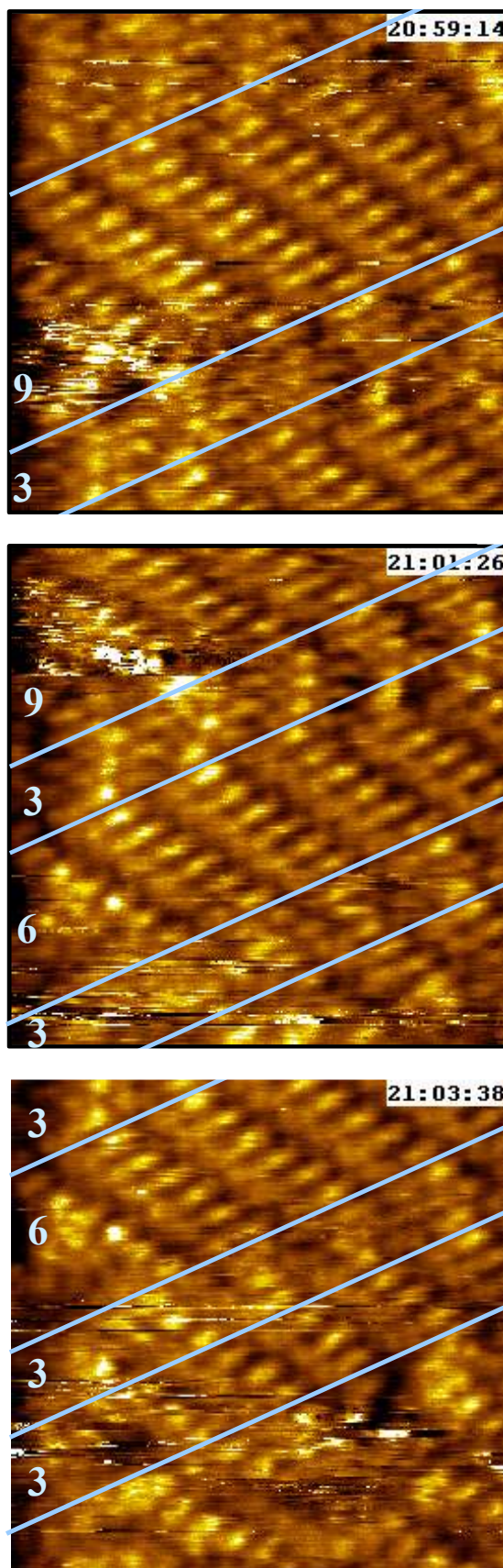

Figure S4: Scans of overlapping regions of PHEN on Au(111). Imaged in aqueous 0.05 M $KClO_4$; tip bias = -0.60 V (vs. the Au(111) substrate), set-point current = 0.85 nA (maximum deviation $\pm$ 10%), and sample potential = 0.08 V vs. SCE.

3. Reductive desorption of the PHEN monolayer

The results of reductive desorption experiments performed for PHEN on a gold electrode in 0.1M $KClO_4$/water solution are described in Fig. S5. The monolayer was formed by exposing the electrode to a solution of 0.36 mM PHEN in water at pH 6.5. This was then washed with water to remove excess PHEN. Figure S6 shows two cyclic voltammograms taken with a time interval of 1 minute, each consisting of four cyclic sweeps of the potential. For each scan the scan rate was 5000 mV s^{-1}. The first scan commenced at point A on Fig. 6 and reveals the reductive desorption of the PHEN monolayer at point B, -1.15 V. Subsequent cycles of this scan reveal no further reductive desorption current. After standing, the cycles were continued from point D, showing a small change E in the signal at –1.15 V. This first cycle was used as a baseline for the reductive desorption shown at point B, and the differences between the first cycles of the two scans, followed by linear baseline correction, is displayed in Fig. 3 and used to determine the monolayer coverage.
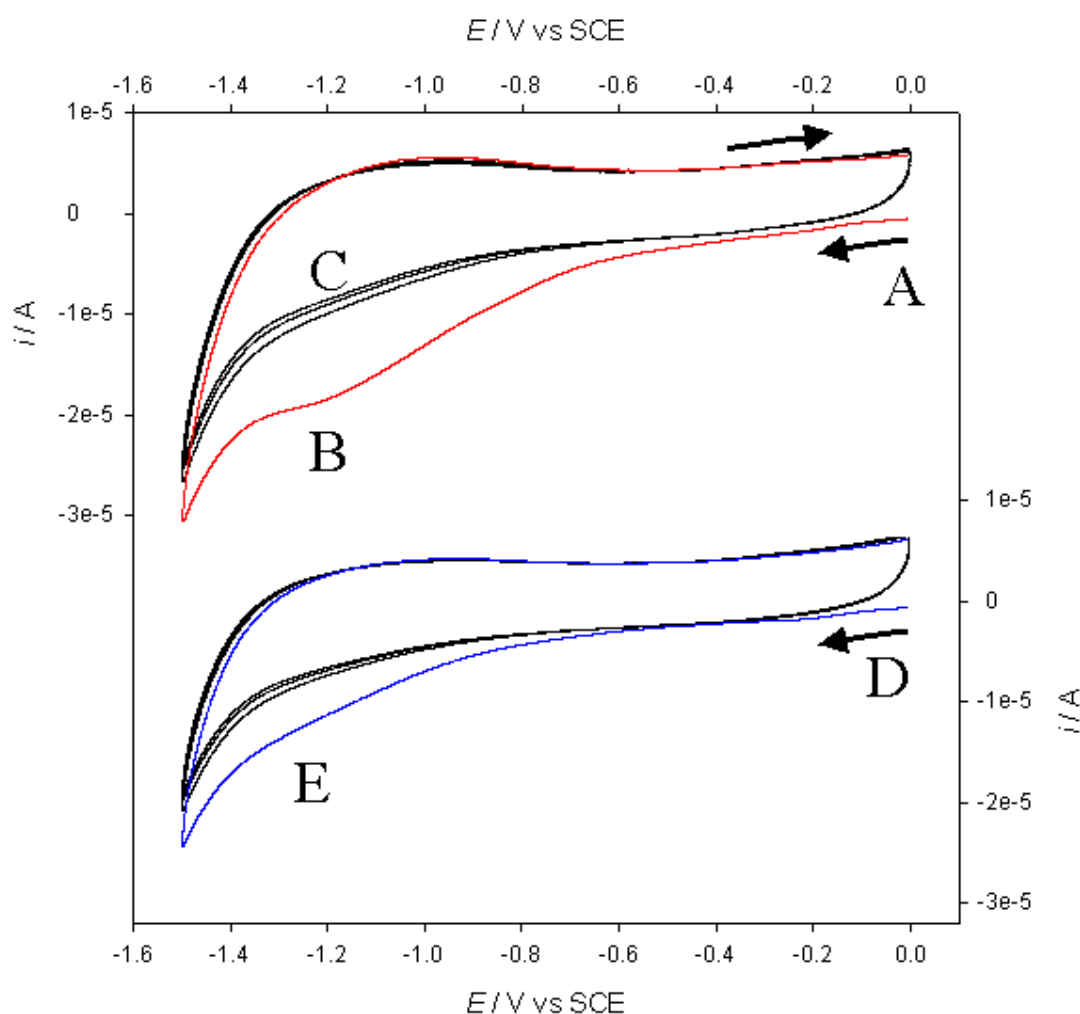

Figure S5: Reductive desorption cyclic voltammetry of PHEN from a gold electrode in 0.1M $KClO_4$/water solution showing 2 scans one minute apart each of 4 cycles The scans start at points A (first scan) and D (second scan), the PHEN layer is removed at stage B.

3. Oxidation of gold surfaces containing PHEN monolayers

The stability of a gold electrode in presence of 1,10-phenanthroline was tested by performing a series of electrochemical experiments where the switch potential, E_λ, was gradually shifted further and further into the anodic potential range. 1,10-phenantrhroline has the ability of stabilizing oxidized gold atoms and thereby lower the potential needed for gold oxidation. From Fig. S6 it can however be seen that no current flow i.e. no oxidation of gold is observed as long as the applied potential do not exceed ca. 0.9V.
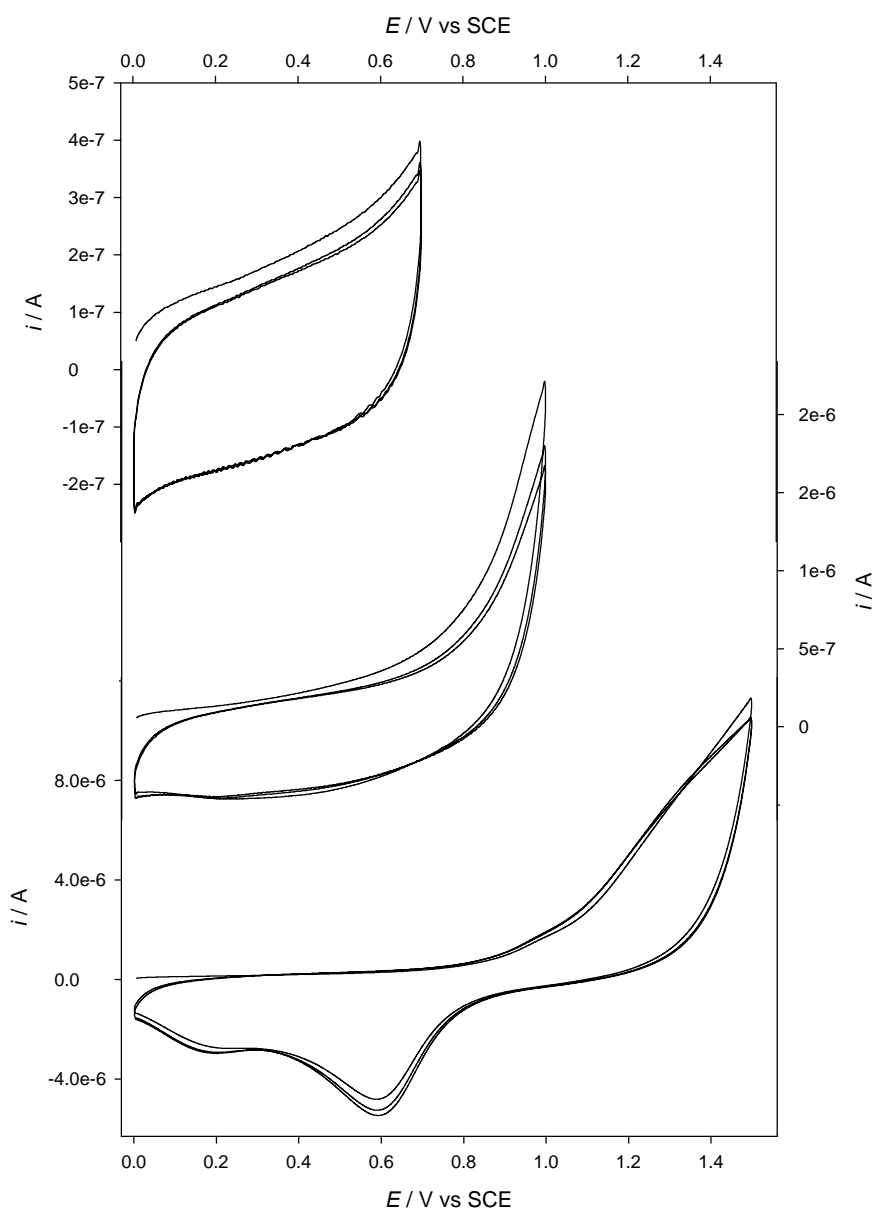

Figure S6: Cyclic voltammograms depicting the response of a gold electrode subjected to a 1,10-phenanthroline/0.1M KClO$_4$ $^{-1}$, switch potentials, E_λ, 0.7 V (top), 1.0 V (middle), and 1.3 V (bottom).